



HAL
open science

Mechanisms of porous dielectric film modification induced by reducing and oxidizing ash plasmas in high-density plasmas

N. Posseme, T. Chevolleau, T. David, Maxime Darnon, O. Louveau, O. R. Joubert

► **To cite this version:**

N. Posseme, T. Chevolleau, T. David, Maxime Darnon, O. Louveau, et al.. Mechanisms of porous dielectric film modification induced by reducing and oxidizing ash plasmas in high-density plasmas. *Journal of Vacuum Science & Technology B, Nanotechnology and Microelectronics*, 2007, 25 (6), pp.1928-1940. <10.1116/1.2804615>. <hal-00397094>

HAL Id: hal-00397094

<https://hal.science/hal-00397094v1>

Submitted on 12 Jan 2024

HAL is a multi-disciplinary open access archive for the deposit and dissemination of scientific research documents, whether they are published or not. The documents may come from teaching and research institutions in France or abroad, or from public or private research centers.

L'archive ouverte pluridisciplinaire **HAL**, est destinée au dépôt et à la diffusion de documents scientifiques de niveau recherche, publiés ou non, émanant des établissements d'enseignement et de recherche français ou étrangers, des laboratoires publics ou privés.



HAL Authorization

Mechanisms of porous dielectric film modification induced by reducing and oxidizing ash plasmas

N. Posseme^{a)}

CEA/LETI-Minatec, 17 Rue des Martyrs, 38054 Grenoble Cedex 09, France

T. Chevolleau^{b)}

CNRS/LTM, CEA/LETI-Minatec, 17 Rue des Martyrs, 38054 Grenoble Cedex 09, France

T. David

CEA/LETI-Minatec, 17 Rue des Martyrs, 38054 Grenoble Cedex 09, France

M. Darnon

CNRS/LTM, CEA/LETI-Minatec, 17 Rue des Martyrs, 38054 Grenoble Cedex 09, France

O. Louveau

STMICROELECTRONICS, Central R&D, 850 Rue J. Monnet, 38926 Crolles Cedex, France

O. Joubert

CNRS/LTM, CEA/LETI-Minatec, 17 Rue des Martyrs, 38054 Grenoble Cedex 09, France

(Received 28 June 2007; accepted 10 October 2007; published 4 December 2007)

This work focuses on the impact of oxidizing and reducing ash chemistries on the modifications of two porous SiOCH films with varied porosities (8% [low porosity (lp)-SiOCH] and 45% [high porosity (hp)-SiOCH]). The ash processes have been performed on SiOCH blanket wafers in either reactive ion etching (RIE) or downstream (DS) reactors. The modifications of the remaining film after plasma exposures have been investigated using different analysis techniques such as x-ray photoelectron spectroscopy, Fourier transform infrared spectroscopy (FTIR), x-ray reflectometry, mercury probe capacitance measurement ($C-V$), and spectroscopic ellipsometry (SE). FTIR analyses show that the lp-SiOCH film is not significantly altered by any of the ash processes investigated (DS-H₂/He, RIE-O₂, and RIE-NH₃), except by downstream oxidizing plasmas (DS-O₂ or DS-N₂/O₂) which induce some carbon depletion and moisture uptake, resulting in a slight increase of the k value. The porosity amplifies the sensitivity of the material to plasma treatments. Indeed, hp-SiOCH is fully modified (moisture uptake and carbon depletion) under oxidizing downstream plasma exposures (DS-O₂ and DS-N₂/O₂), while it is partially altered with the formation of a denser and modified layer (40–60 nm thick), which is carbon depleted, hydrophilic, and composed of SiO_xN_yH_z with RIE-NH₃ and DS-N₂/H₂ plasmas and SiO_xH_y with RIE-O₂ plasma. In all the cases, the k value increase is mainly attributed to the moisture uptake rather than methyl group consumption. hp-SiOCH material is not altered using reducing DS chemistries (H₂/He and H₂/Ar). The porous SiOCH film degradation is presented and discussed with respect to chemistry, plasma parameters, and plasma mode in terms of film modification mechanism. © 2007 American Vacuum Society. [DOI: 10.1116/1.2804615]

I. INTRODUCTION

The most serious challenges in semiconductor manufacturing are to produce low cost integrated circuits (ICs) with increasing integration densities and to develop high performance devices. An important problem that we are facing today is that electric signal propagation through metal interconnects is delayed by the resistance (R) in the metal lines and the capacitance (C) between adjacent metal lines. Several solutions are being considered to maintain or reduce the RC delay in an effort to optimize the performance of ICs with a higher packing density. One of the ways to decrease the run time delay and thus the RC product is to use lower dielectric constant materials.

For the 32 nm technology node and below, the International Technology Roadmap for Semiconductors requires the integration of dielectric materials, such as SiOCH or methyl silsesquioxane films, with effective k values between 1.8 and 2.1.¹ To achieve this target, porosity is introduced into dielectric materials. However, the porosity brings in serious issues since the main integration difficulties with such materials are their sensitivity to etch and ash plasma exposures leading to a change of the film structural properties (a film modification is usually observed during an ash plasma exposure). For instance, O₂-based ash plasmas tend to oxidize SiOCH films converting the top layer into a hydrophilic SiO₂-like material^{2–7} generating a strong increase of the dielectric constant. In order to reduce this type of damage, several groups have focused their efforts on damage-free ashing plasmas using reducing chemistries.^{2,3,8,9}

^{a)}Electronic mail: nicolas.posseme@st.com

^{b)}Electronic mail: thierry.chevolleau@cea.fr

TABLE I. Material properties of the hp- and lp-SiOCH films.

Material	Deposition method	Porosity (%)	Density (g cm ⁻³)	Dielectric constant	Refractive index (632.8 nm)
hp-SiOCH	Spin coating	45	0.9	2.2	1.25
lp-SiOCH	PECVD	8	1.2	2.9	1.42

This study is dedicated to the understanding of the modifications of SiOCH low- k materials induced by oxidizing and reducing ash chemistries. Two different materials have been studied: a SiOCH material presenting a low porosity ($k=2.9$, 8% porosity) and a SiOCH material presenting a high porosity ($k=2.2$, 45% porosity). We have compared the modifications induced by two types of plasma modes, either reactive ion etching (RIE) or downstream (DS). The modifications of the remaining film after plasma exposures have been investigated using different analysis techniques such as x-ray photoelectron spectroscopy (XPS), Fourier transform infrared spectroscopy (FTIR), x-ray reflectometry (XRR), mercury probe capacitance measurement ($C-V$), and spectroscopic ellipsometry (SE).

II. EXPERIMENT

A. Dielectric materials

In this study, we have used 200 mm diameter silicon wafers coated with either 300 nm thick porous SiOCH material (45% porosity with open porosity) from JSR (LKD-5109TM) deposited by spinning or a 300 nm thick SiOCH material from Applied Materials (Black DiamondTM) deposited by plasma enhanced chemical vapor deposition (PECVD). The latter has generally been considered as a dense SiOCH material¹⁰ but some porosimetric studies have demonstrated that it presents a microporosity of 8%.¹¹

In this paper, the porous material from JSR will be referenced as high porosity hp-SiOCH and the material from Applied Materials as low porosity lp-SiOCH. The main properties of these materials are described in Table I.

B. Photoresist ashers and plasma chemistries

Processes have been carried out either in a magnetically enhanced RIE (MERIE) eMaxTM from Applied Materials using O₂ and NH₃ medium density plasmas (MERIE mode) or in a photoresist Novellus PEP IRIDIATM microwave stripper using various oxidizing and reducing chemistries [H₂/He (3:1), H₂/Ar (3:1), N₂/H₂ (3:1), O₂, and N₂/O₂ (3:1)] (downstream mode).

1. RIE mode

The eMaxTM reactor generates capacitively coupled plasmas. The wafer sits on an electrode powered with a rf generator operating at 13.56 MHz in a power range between 100 and 2000 W. The reactor is surrounded by four electromagnets producing a rotating magnetic field (0.5 Hz, 0–200 G) leading to an increase in plasma density. In this study, the

reactor has only been operated in RIE mode: the magnetic field is switched off (0 G). The pressure in the chamber is set at 75 mTorr and 80 mTorr (for O₂ and NH₃, respectively) by a motorized throttle valve and the power is set at 200 W and 350 W (for O₂ and NH₃, respectively). Wafers are clamped using an electrostatic chuck and the wafer temperature is kept constant at 15 °C by a helium back side regulation.

Before each experiment, a cleaning process (O₂ plasma) using a blanket silicon wafer and a conditioning process are performed in order to generate reproducible chamber conditions from wafer to wafer. Typical blanket resist ash rates are 300 and 150 nm min⁻¹ for RIE-O₂ and RIE-NH₃ chemistries, respectively (Table II). Both ash chemistries do not induce any loss of lp-SiOCH materials, while hp-SiOCH etch rates of 20 and 10 nm min⁻¹ are measured during the exposure to the same ashing plasmas.

2. Downstream mode

The Novellus PEP IRIDIATM photoresist stripper features DS microwave plasma (2450 MHz) and rf biased platen (13.56 MHz). The substrate temperature is controlled by infrared lamp heating. For this study, the substrate temperature is set at 270 °C and the downstream mode has only been used. In these conditions, Louveau *et al.* have shown that hydrogen-based plasma treatment is benign to the hp-SiOCH material and efficient in terms of resist removal rate.³

Before each run of plasma, a conditioning process on a blanket resist wafer is performed in order to generate reproducible chamber conditions from wafer to wafer. Besides, pump/purge steps are included into recipes (especially reducing chemistries) to avoid any possible air contaminations. The ash rates, reported in Table II, are estimated at around 150 nm min⁻¹ with all the reducing chemistries in the down-

TABLE II. Ash rate as a function of plasma mode (downstream or RIE) and chemistry.

	Ash rate (nm min ⁻¹)	
H ₂ /Ar (3:1)	155	Downstream
H ₂ /He (3:1)	150	Downstream
H ₂ /N ₂ (3:1)	160	Downstream
O ₂	>1 μm	Downstream
O ₂ /N ₂ (3:1)	>1 μm	Downstream
O ₂	300	RIE
NH ₃	150	RIE

stream mode (DS-H₂/Ar, DS-H₂/He, and DS-N₂/H₂). For oxidizing downstream plasmas, the ash rate is one order of magnitude higher ($>1 \mu\text{m min}^{-1}$).

Furthermore, the different ash chemistries investigated do not consume the lp-SiOCH material, while etch rates of 80 and 20 nm min⁻¹ are measured for hp-SiOCH film after exposition to oxidizing (with or without nitrogen) and DS-N₂/H₂ ash chemistries, respectively. Reducing chemistries without nitrogen (DS-H₂/He and DS-H₂/Ar) do not consume the hp-SiOCH.

For the experiments presented in next sections, all process durations are performed with a step time adapted to remove 150 nm postetch remaining resist. Therefore, the process time is set at 60 s for reducing plasmas, whereas the time is set at 30 s for all oxidizing chemistries.

C. Film characterization

After plasma exposure, modifications of the remaining dielectric layers are investigated by several techniques listed and presented below.

1. Optical properties: Spectroscopic ellipsometry

The refractive index and the thickness of the films are measured *in situ* after ashing treatment by using UVISSEL (ISA Jobin Yvon) and *ex situ* using KLA-Tencor SE1280 spectroscopic ellipsometers. To determine the refractive index and the film thickness, the ellipsometry parameters are fitted with a nonabsorbent Cauchy model for the lp-SiOCH and with a Bruggeman medium effective approximation assuming a homogeneous mixture of nonabsorbent Cauchy material and void for the hp-SiOCH.

2. Bulk analyses: Infrared spectroscopy

FTIR has been used in the transmission mode with a Bio-Rad FTIR spectrometer model QS-500 recording spectra between 400 and 4000 cm⁻¹ using a 2 cm⁻¹ spectral resolution and an average of 32 scans. The FTIR absorbance spectra presented in the next sections are normalized to the dielectric film thickness remaining after plasma exposure.

3. Surface analyses: X-ray photoelectron spectroscopy

The XPS analyses can be carried out under quasi-*in situ* conditions via a vacuum transfer of the 200 mm wafer into the XPS chamber after processing in the etch chamber. Nevertheless, XPS analyses presented in the next sections have been performed after air exposure. The spectra are collected with a Fisons Surface Systems ESCALAB 220i operating with an Al K α x-ray source ($h\nu=1486.6 \text{ eV}$) and an electron energy analyzer operating in a constant pass energy mode of 20 eV. Chemical compositions are derived from the areas of the different XPS spectra. The sum of the different surface element atomic concentrations is equal to 100%. The hydrogen content is not taken into account in this calculation since hydrogen cannot be detected by XPS. More details of the

experimental characterization conditions can be found elsewhere.^{12,13}

4. Density and thickness evolution: X-ray reflectometry

XRR analyses have been performed *ex situ* on 200 mm wafers. The apparatus is a J VX5200 from Jordan Valley using a Cu K α x-ray source ($\lambda=0.154 \text{ nm}$) for excitation and an array of solid state x-ray detectors for measurement.¹⁴ The XRR technique, using an x-ray beam at grazing angle, is a nondestructive method, which gives information on the thickness and density of the material. In fact, the measurement of the critical angle (angle below which the reflection is total) is related to the electronic density of the top layer.¹⁵ An increase of the critical angle is, therefore, representative of an increase in surface density. The measurement of the interference fringe period allows the determination of the material thickness.

5. Capacitance measurement: Mercury probe

The dielectric constant of blanket films has been calculated before and after the different plasma exposures using capacitance-voltage (*C-V*) measurements at 0.1 MHz. *C-V* measurements have been performed using a mercury probe capacitance measurement (*C-V*) system (model SSM495).

III. RESULTS

A. Pristine films analyses

As-deposited films have been analyzed by XPS and FTIR before plasma exposures. The XPS survey spectra of both as-deposited lp-SiOCH and hp-SiOCH, presented in Fig. 1(a), show the presence of silicon, oxygen, and carbon. The surface composition, reported in Table III, shows that the lp-SiOCH is composed of Si (35%), O (39%), and C (26%), while the hp-SiOCH exhibits a lower carbon content, Si (37%), O (50%), and C (13%).

FTIR analyses, shown in Fig. 2, indicate that the as-deposited film spectra have main absorption bands at 1035 and 1056 cm⁻¹ for the lp-SiOCH and hp-SiOCH, respectively, corresponding to the Si-O-Si stretching vibration mode. Based on previous studies, this difference in SiOSi peak positions is attributed to a change in the Si-O-Si bonding angle and/or to a lower carbon content in the films.¹⁶⁻¹⁹ This is in good agreement with the surface composition determined by XPS (reported in Table III) since the Si-O-Si peak position decreases to lower wave numbers when the carbon concentration in the film increases (26% of carbon in the lp-SiOCH film, while the hp-SiOCH has 13% carbon content). Two additional peaks are also observed at 1275 and 2960 cm⁻¹, which are assigned to the Si-CH₃ and C-H₃ vibration modes, respectively. Based on these FTIR reference spectra, both as-deposited (hp- and lp-) SiOCH films consist of a siloxane (Si-O-Si) network terminated by methyl groups (Si-CH₃).

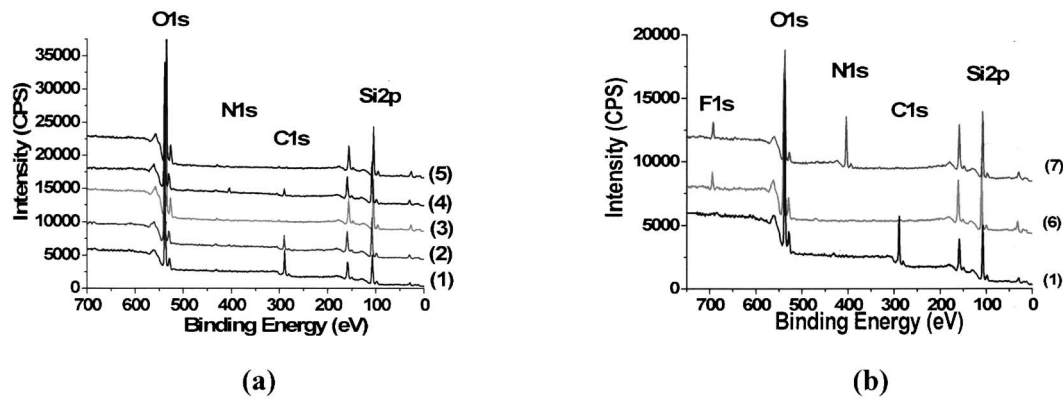


FIG. 1. lp- and hp-SiOCH survey spectra performed in (a) downstream (DS) mode and (b) RIE mode obtained for different plasma conditions, (1) pristine, (2) H₂/Ar and H₂/He, (3) O₂ and N₂/O₂, (4) H₂/N₂ (lp-SiOCH only), (5) O₂ and H₂/N₂ (hp-SiOCH only), (6) O₂, and (7) NH₃.

B. Dielectric films after ashing treatments

1. Surface analysis

Figure 1(a) shows the impact of the different DS chemistries on both lp-SiOCH and hp-SiOCH film surface modifications through XPS survey spectra. After the different ash processes, Fig. 1(a) shows no other contribution except for the DS-N₂/H₂ ash chemistry, where a new peak is detected at 399 eV and assigned to nitrogen bonded to silicon.^{12,13} The surface compositions obtained after the different ash chemistries exposure are summarized in Table III. H₂/He and H₂/Ar downstream reducing chemistries lead to a carbon loss of 40% in the first 10 nm (thickness probed by XPS) of both lp-SiOCH and hp-SiOCH top surfaces with respect to the pristine films. A higher carbon depletion (60%) is observed at the surface of the lp-SiOCH when it is exposed to the downstream oxidizing plasma (DS-O₂), while a carbon-free surface is detected for the hp-SiOCH. N₂ addition to H₂ and O₂ downstream plasmas induces stronger carbon depletions (60% and 90%, respectively) at the lp-SiOCH film surface. In this case, no more carbon is detected at the hp-SiOCH film surface.

The whole results show that oxidizing chemistries induce a stronger surface carbon depletion than reducing chemistries in the downstream mode. These surface analyses also high-

light that the N₂ addition combined with high porosity SiOCH materials in both oxidizing and reducing chemistries favors the carbon removal at the near surface.

After RIE plasma exposures (RIE-O₂ and RIE-NH₃), lp-SiOCH and hp-SiOCH XPS survey spectra, represented in Fig. 1(b), show that the surface is fully carbon depleted. A new peak contribution is located at 688 eV and assigned to fluorine.^{12,13} This small amount of fluorine (2%–5%) originates from the memory effect of the fluorine present on the reactor walls when using fluorocarbon plasmas. Small concentrations of fluorine are still present on the chamber walls even if RIE-O₂ plasmas are used to clean the chamber before the ash process. After RIE-NH₃ plasma exposure, nitrogen atoms bonded to silicon are detected at the lp-SiOCH and hp-SiOCH film surfaces. In these conditions, the nitrogen concentrations are about 6% and 10% for the lp-SiOCH and hp-SiOCH, respectively (see Table III).

These results show that after RIE plasma and air exposures, the surface is fully carbon depleted with both oxidizing and reducing chemistries. A nitrogen containing surface is observed on both low-*k* materials with the NH₃ chemistry. These XPS analyses only provide information on film modi-

TABLE III. Surface composition determined by XPS of the hp- and lp-SiOCH after different ash plasma exposures.

	lp-SiOCH composition	hp-SiOCH composition
Pristine film	35% Si, 39% O, 26% C	37% Si, 50% O, 13% C
DS-H ₂	37% Si, 46% O, 16% C	38% Si, 51% O, 11% C
DS-N ₂	33% Si, 43% O, 21% C, 2% N	37% Si, 50% O, 12% C, 1% N
DS-O ₂	35% Si, 55% O, 10% C	40% Si, 60% O
DS-H ₂ /Ar	40% Si, 46% O, 14% C	40% Si, 52% O, 8% C
DS-H ₂ /He	40% Si, 46% O, 14% C	40% Si, 52% O, 8% C
DS-N ₂ /H ₂	40% Si, 52% O, 6% C, 2% N	40% Si, 58% O, 2% N
DS-N ₂ /O ₂	40% Si, 58% O, 2% C	37% Si, 63% O
RIE-O ₂	35% Si, 60% O, 5% C	44% Si, 50% O, 6% F
RIE-NH ₃	38% Si, 50% O, 3% C, 3% F 6% N	42% Si, 46% O, 2% F, 10% N

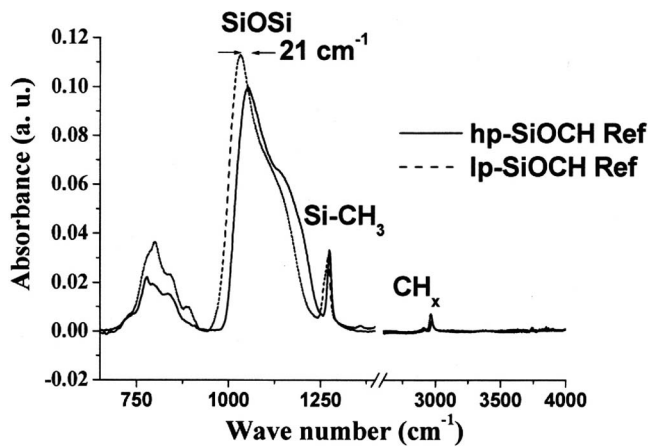


Fig. 2. FTIR spectra comparison between the pristine lp- and hp-SiOCH films.

fications occurring at the near surface. Is this modification only located at the near surface or does it extend deeper in the SiOCH films?

2. Bulk analysis

The (hp- and lp-) SiOCH structural film modifications after ash processes have been investigated by infrared spectroscopy. Figure 3 shows the comparison between lp-SiOCH spectra [Fig. 3(a)] and hp-SiOCH spectra [Fig. 3(b)] after exposure to the different plasmas.

a. *lp-SiOCH after plasma treatments.* After exposure to reducing and oxidizing chemistries in both DS and RIE plasma modes, FTIR spectra [see Fig. 3(a)] exhibit almost the same vibration modes as the pristine material ones. The normalized absorbance is identical and no other vibration bands are observed except after DS oxygen-based plasma exposure (O_2 and N_2/O_2). This indicates that most of the investigated ash processes do not induce a noticeable bulk modification. When using downstream oxygen-based plasmas (with or without nitrogen), additional weak absorption bands are observed. These peaks, localized between 3000 and 3700 cm^{-1} , are assigned to isolated associated hydroxyl O–H and water groups, which indicate moisture uptake.^{12,13}

The presence of hydroxyl groups is also confirmed by a new absorption peak localized at 960 cm^{-1} that is attributed to Si–O–H bonds.^{12,13} In these conditions, the normalized FTIR spectra also exhibit a change in Si–O–Si and Si–CH₃ peak intensities with respect to the as-deposited material.

The carbon content in the film can be monitored by calculating the SiCH₃/SiOSi peak area ratio from the FTIR spectra.¹⁹ In our experimental conditions, the carbon depletion measurement can be compared from one sample to another since the remaining film thickness after plasma exposure is almost similar to the pristine film one. After DS- O_2 and DS- N_2/O_2 ash plasma exposures, the relative carbon content decreases by about 10%, which is well correlated with the carbon depletion detected at the near surface by XPS. In the meantime, a slight shift in the peak position of Si–O–Si bonds is observed from 1035 to 1065 cm^{-1} . Dielectric constant measurements for the lp-SiOCH have been performed after plasmas. The dielectric constant (k) slightly increases after RIE (O_2 and NH_3) and DS reducing ash processes from 2.9 up to 3.1. A higher increase in the k value (up to 3.3) is observed after DS- O_2 and DS- N_2/O_2 ash processes, indicating a higher degradation of the remaining film, which is in good agreement with the bulk modification previously observed by FTIR. These results show that the lp-SiOCH film is not significantly altered by any of the ash process investigated, except by downstream oxidizing plasmas which tend to induce some carbon depletion and moisture uptake resulting in a slight increase of the k value.

b. *hp-SiOCH after plasma treatments.* Figure 3(b) shows that the normalized absorbance of the hp-SiOCH after H_2/He or H_2/Ar downstream plasma exposures is the same as the pristine film one: no carbon depletion and no other vibration bands are detected. When nitrogen is added to the hydrogen-based chemistry, FTIR spectra reveal a new absorption band between 3000 and 3700 cm^{-1} , assigned to isolated and associated hydroxyl OH and water groups. In the meantime, a SiOSi peak shift to higher wave numbers (+7 cm^{-1}) is detected, which is related to a carbon depletion estimated at about 35% (see Fig. 4). These results underline that only nitrogen-free reducing downstream plasmas do not induce bulk modifications of the hp-SiOCH. After exposure

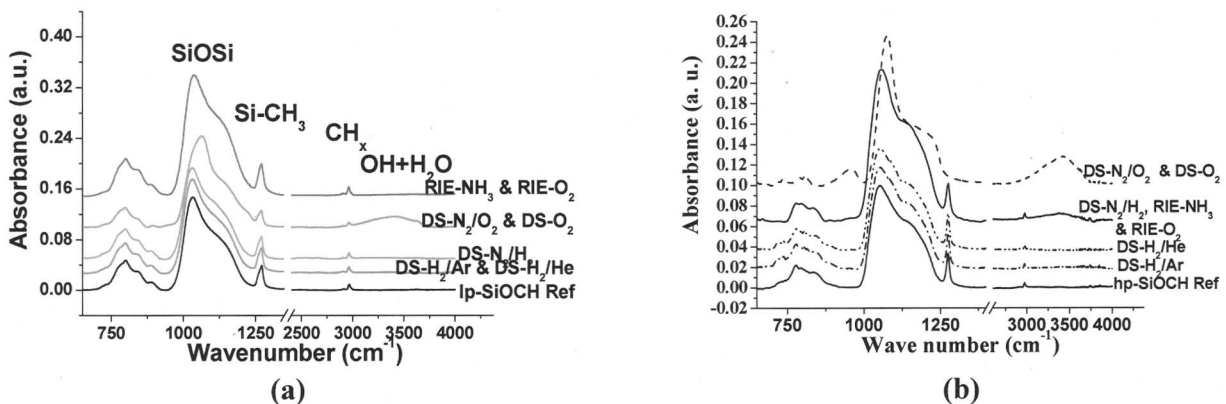


Fig. 3. FTIR spectra of (a) lp- and (b) hp-SiOCH films after various plasma conditions.

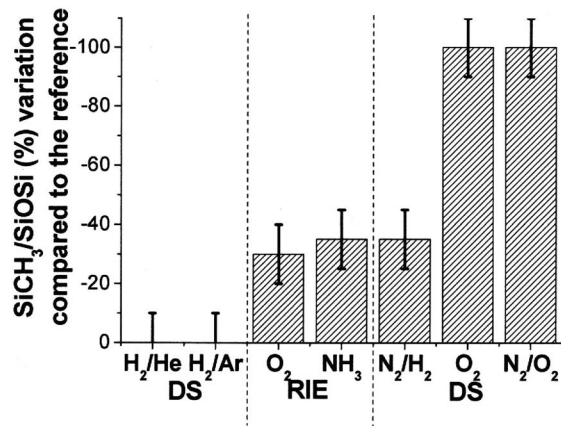


FIG. 4. Impact of downstream and RIE plasmas on methyl group consumption of the hp-SiOCH.

to oxidizing downstream plasmas (O₂ and N₂/O₂), FTIR spectra show a large absorption band between 3000 and 3700 cm⁻¹ with no methyl vibration bands and an important shift of the SiOSi peak to higher wave numbers (+23 cm⁻¹). This behavior shows that the highly porous film is deeply altered by oxidizing plasmas leading to an important moisture uptake (H₂O and SiOH groups) and a complete carbon depletion. After exposure to RIE plasmas, O₂ and NH₃, FTIR spectra reveal the presence of isolated associated hydroxyl OH and water groups. A slight shift of the SiOSi peak of +7 cm⁻¹ is also observed associated with a 30%–35% decrease in the SiCH₃/SiOSi peak area ratio (as shown in Fig. 4). These results indicate that the hp-SiOCH film is modified with a partial carbon depletion and moisture uptake.

In summary, a complete bulk modification of the hp-SiOCH is observed under oxidizing downstream plasma exposure (O₂, N₂/O₂), whereas no noticeable degradation is detected with nitrogen-free downstream reducing chemistries (H₂/He and H₂/Ar). Contrary to lp-SiOCH films where the modification is limited at the film surface, a partial bulk modification is observed after hp-SiOCH exposure to reducing and oxidizing RIE plasmas and N₂/H₂ downstream plasmas. How deep is the film modification?

3. Depth modification of the hp-SiOCH film

In order to estimate the thickness of the modified layer after exposures to DS-N₂/H₂, RIE-O₂, and RIE-NH₃ ashing plasmas, we have exposed blanket hp-SiOCH films to successive diluted fluorhydric acid (HF) dips (0.1%) every 10 s. The remaining thickness and refractive index are measured by *ex situ* ellipsometry after each HF dip. These experiments rely on the principle that the pristine hp-SiOCH is not consumed during the HF dip, while the modified layer (with moisture uptake and carbon depletion) is removed. For samples treated with RIE-O₂, RIE-NH₃, and DS-N₂/H₂ plasmas, Fig. 5 shows that the refractive index decreases down to its reference value after 20 and 60 s of HF dips, respectively. Then, it becomes stable for further exposure times (the remaining film is not consumed anymore). Concerning the surface density, XRR measurements indicate critical angles of

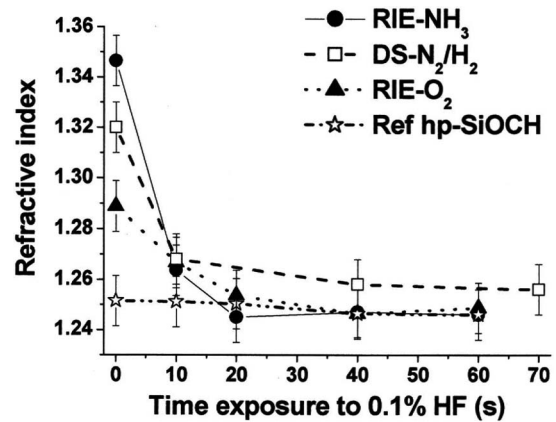


FIG. 5. Refractive index variation of the hp-SiOCH vs time exposure in HF solution after different plasma conditions.

0.17° and 0.165° after RIE-O₂ and RIE-NH₃ plasma treatments, respectively. After HF dip, Fig. 6 shows that the critical angle is reset to the value of the pristine material (i.e., 0.14°). Therefore, the evolution of the critical angle reveals (i) that the surface density of the material is increased by ash plasma exposure and (ii) that the density of the material under the modified layer is unchanged with respect to the pristine film. Both refractive index and critical angle measurements clearly indicate that the hp-SiOCH film is not fully altered by exposure to those ashing processes. The remaining SiOCH film after plasma can, therefore, be modeled as a damaged layer (carbon depleted, denser, and hydrophilic) over a hardly modified hp-SiOCH layer. Based on ellipsometry results depicted in Fig. 5, damaged layer thickness can be estimated to be about 40–45 nm with RIE-O₂ plasma and 60 nm with DS-N₂/H₂ and RIE-NH₃ plasmas. These measurements are confirmed with XRR analyses which estimate the thicknesses removed by HF dip to 37 and 62 nm with RIE-O₂ and RIE-NH₃, respectively.

As previously shown, the methyl group consumption of 30%–35% in the hp-SiOCH film after the different RIE plasma exposures is well correlated with a 7 cm⁻¹ SiOSi peak shift to higher wave numbers. Besides, XPS analyses show that the surface is carbon-free after exposure to ashing

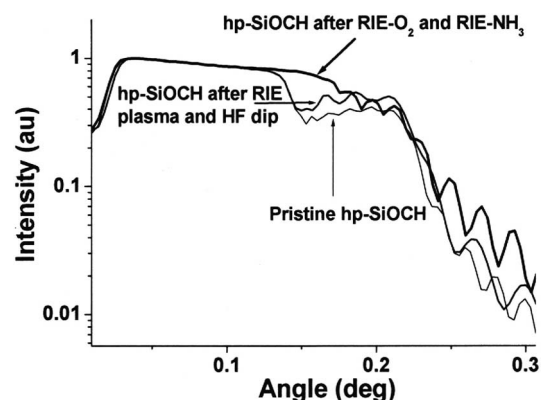


FIG. 6. hp-SiOCH XRR spectra before and after RIE ash plasmas and HF dip.

TABLE IV. hp-SiOCH surface composition determined by XPS after ash plasma processes and 60 s diluted HF (0.1%) dip.

	hp-SiOCH surface composition	Surface composition after HF (0.1%) dip
Pristine film	37% Si, 50% O, 13% C	37% Si, 50% O, 13% C
DS-N ₂ /H ₂	40% Si, 58% O, 2% N ₂	37% Si, 52% O, 11% C
RIE-O ₂	44% Si, 50% O, 6% F	37% Si, 55% O, 8% C
RIE-NH ₃	42% Si, 46% O, 10% N, 2% F	37% Si, 53% O, 10% C

processes (no C–Si bonds are detected by XPS). Thus, the damaged layer can be considered as a SiO_xH_y-like film with the RIE-O₂ plasma and a SiO_xN_yH_z-like film with RIE-NH₃ and DS-N₂/H₂ plasmas (see XPS results summarized in Table IV).

After RIE ashing plasma exposures (O₂ and NH₃) and 60 s of diluted HF dip, FTIR analyses (see Fig. 7) show that the carbon content and the SiOSi peak position are close to the pristine film ones. However, even if the structural properties of the remaining hp-SiOCH after HF dip and pristine films are close, a broad absorption band between 3000 and 3700 cm⁻¹ is still detected, indicating a slight moisture uptake.

In summary, the hp-SiOCH film is partially altered after RIE-O₂, RIE-NH₃, and DS-N₂/H₂ plasmas. The surface is hydrophilic and denser than the pristine material, and the composition of the damaged layer is SiO_xH_y after RIE-O₂ or SiO_xN_yH_z after DS-N₂/H₂ and RIE-NH₃ plasma treatments. The depths of modification are estimated to be about of 40 nm after RIE-O₂ and 60 nm after RIE-NH₃ and DS-N₂/H₂ plasma exposures. The remaining low-*k* material underneath the damaged layer exhibits similar properties to the as-deposited material, excepting a slight moisture uptake.

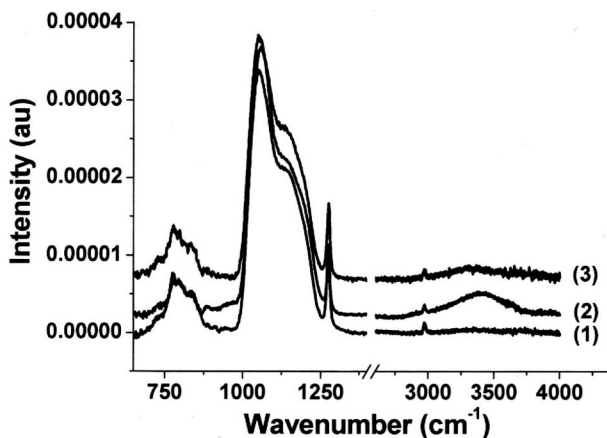


FIG. 7. Comparison of the hp-SiOCH FTIR spectra after various conditions: (1) pristine film, (2) RIE ash plasma (O₂ or NH₃), and (3) RIE processes and 60 s HF dip.

4. Dielectric constant measurement

After DS-H₂/He and DS-H₂/Ar ash process exposures, the *k* values of the hp-SiOCH film measured by the mercury probe capacitance are identical to the pristine material one. These results tend to confirm that the hp-SiOCH material is not altered using such reducing chemistries. On the contrary, the *k* value increases from 2.2 to 2.5, 2.8, and 3.2 when exposed to RIE-NH₃, RIE-O₂, and DS-N₂/H₂ ash processes, respectively. The *k* value increase is related to the film modifications induced by the ash processes.

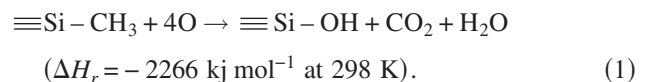
IV. DISCUSSION

The experiments performed in the previous sections describe the impact of reducing- and oxidizing-based ash plasmas on the lp-SiOCH and hp-SiOCH film modifications. The following section goes deeper into details in order to understand how the films are modified as a function of the ash chemistry and how these modifications may affect the *k* value.

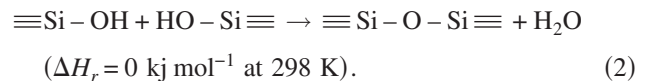
A. O₂ plasma

The effect of oxygen plasma on porous dielectric film modification has been widely studied in the literature. It has been shown that O₂-based ashing plasmas tend to oxidize SiOC(–H) films converting the top layer into a hydrophilic SiO₂-like material.^{2–7}

Oxygen reactive species can deeply diffuse into the film through its porosity and react with –H or methyl –CH₃ groups, which are bonded to the Si atoms of the SiOSi material network, producing Si–OH bonds through the following reactions as proposed by Chang *et al.*²⁰



Hydrophilic SiOH groups can either induce moisture absorption or react between each other to form SiOSi absorption band as the following reaction:



These reactions are strongly dependent on the plasma operating conditions since Worsley *et al.* have shown that the depth of the perturbation induced by the O₂ ashing plasma increases with either higher oxygen reactive species concentration or higher substrate temperature.²¹ In our work, XPS and FTIR analyses reveal that both lp- and hp-SiOCH materials are damaged under downstream oxidizing plasma exposures. The main difference between materials is the lower loss of methyl groups in the lp-SiOCH compared to the hp-SiOCH, which is fully carbon depleted. The methyl group removal is correlated with an important absorption band assigned to isolated associated hydroxyl O–H and water groups detected and silanol groups detected in both materials. The SiOSi peak position simultaneously shifts to higher energies

with carbon depletion. These analyses demonstrate the correlation between the film modification and the porosity of the material.²¹

When the wafer is bombarded by energetic ions (RIE mode), oxygen reactive species and oxygen ions react with methyl groups leading to the formation of a 40–45 nm thick carbon depleted layer with the hp-SiOCH film, while the carbon depletion is limited at the top surface in the lp-SiOCH film. A lower film depth modification has been detected when the hp-SiOCH material is exposed to O₂ RIE plasmas than that to O₂ DS plasmas. However, the impact of O₂ plasmas performed in DS or RIE mode is difficult to compare since the plasma conditions are strongly different (reactive species concentrations, ion bombardment energy, and wafer temperature). We have performed complementary analyses to bring new insight on the impact of the oxygen concentration, wafer temperature, and ion bombardment energy on the hp-SiOCH film modification exposed to O₂ RIE plasmas.

1. Impact of the ion bombardment energy on the film modification

In a RIE reactor, separating the contribution from oxygen radicals and oxygen ions cannot be achieved, since ion energy and radical density are simultaneously controlled by the plasma power. However, by using a simple technique developed by Joubert *et al.*, we can get some interesting information on the respective roles of ions and neutrals on the film modification in the RIE chamber.²²

The samples used to study the impact of the ion bombardment on the hp-SiOCH film modification are made of a 200 nm thick hp-SiOCH film deposited on a silicon wafer, which is then cut in square pieces of about 6 cm². The piece of sample can then be stuck (directly on the wafer) or raised (surelevated) onto a 200 mm diameter SiO₂ wafer. Stuck coupons withstand the same plasma conditions as blanket wafers (i.e., high energy ion bombardment). Raised coupons are surelevated, thanks to four cylindrical rolls made of adhesive Kapton™. The coupon is, therefore, separated from the wafer by a “gap.” The thickness of the gap is calculated to prevent the dc biasing of the hp-SiOCH coupon. A theoretical calculation shows that the required gap thickness to maintain the sample electrically floating strongly depends on the electron plasma density (n_e) and the dc self-bias voltage applied to the wafer.²²

We have shown that a gap thickness of about 6 mm is required in the eMax™ etcher (plasma density $n_e \leq 10^{11}$ cm⁻³) in order to prevent the dc self-bias of the hp-SiOCH sample.²³ Since the ions bombarding the sample have an energy of $e(V_p - V_f)$, where V_p is the plasma potential and V_f the floating potential, typically a few tens of eV, the raised hp-SiOCH coupon withstands identical plasma conditions as the stuck coupon, excepting that the ion energy is much lower. The effects of oxygen radicals and ion energy are then decorrelated. The temperature of the floating hp-SiOCH sample has been monitored, thanks to temperature sticks protected from direct plasma exposure by Kapton™. It

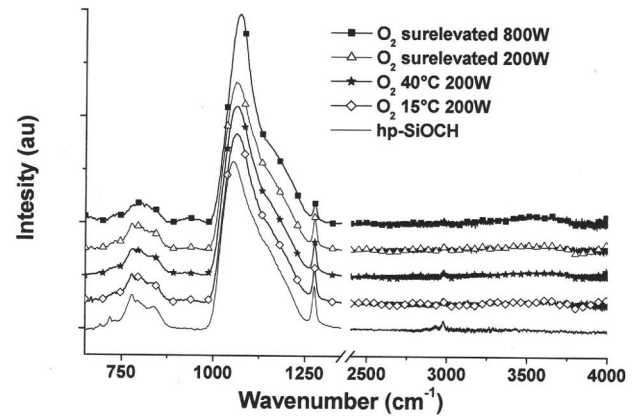


FIG. 8. Effect of RIE-O₂ plasmas on the hp-SiOCH FTIR spectrum for different plasma conditions.

has shown that the temperature of the floating hp-SiOCH sample is maintained below 40 °C during the ashing process. However, an increase in temperature from 15 °C (temperature of the stuck coupon) to 40 °C (temperature of the raised coupon) could play a significant role on the hp-SiOCH film modification. We have, therefore, monitored by FTIR the impact of the temperature on the modification of stuck hp-SiOCH coupons in O₂ plasmas (rf power of 200 W) at the two different chuck temperatures mentioned above: 15 and 40 °C (see Fig. 8 showing the FTIR spectra). Figure 8 shows that the FTIR spectra are quite identical in that range of temperatures, with a carbon depletion of 30%, a peak position shift of 10 cm⁻¹, and a very low amount of moisture uptake. The hp-SiOCH film consumption is around 10 nm for both substrate temperatures. These results show that the temperature of the floating sample (<40 °C) is not a key parameter on the material modification. Thanks to this result, we can estimate the consequence of the ions energy on the material modification by comparing the similar O₂ plasmas performed with a power set at 200 W on the stuck sample (impact of chemistry and high energy ion bombardment) and on the floating sample (impact of chemistry and low energy ion bombardment). Under high energy ion bombardment (when the sample is stuck), the carbon depletion estimated by FTIR is about 30%. When the sample is floating, the carbon depletion is about 33%. The shifts in peak positions are 10 and 8 cm⁻¹ under high energy ion and low energy ion bombardments, respectively. This comparison shows that the ion energy has little impact on the hp-SiOCH film modification.

In the literature, two articles have reported a relatively lower degradation of porous materials during the oxygen plasma exposure when the substrate is biased.^{9,24} In these papers, the assumption is made that the physical impact of the ion bombardment generates a degradation of the material through a methyl -CH₃ group depletion. In the proposed mechanism, the oxygen ions remove the modified layer as it forms due to the high chemical sputtering rate of material induced by the oxygen plasma. However, in our experimental conditions, the hp-SiOCH film consumptions, under high

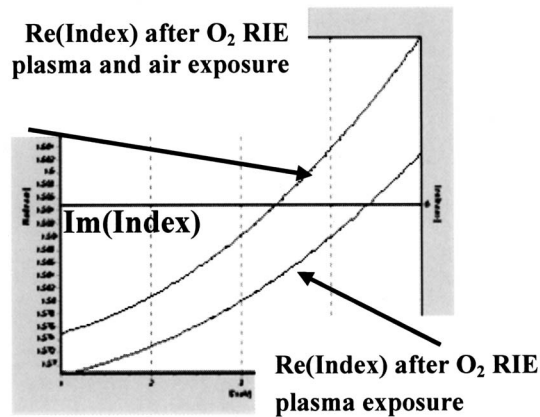


FIG. 9. Effect of air exposure on refractive index variation of the hp-SiOCH exposed to RIE-O₂ plasma.

and low ion energy bombardment conditions are only about 10 and 3 nm, respectively. Therefore, this very limited hp-SiOCH consumption shows that in our case, the removal rate of the material is low and cannot play a significant role in decreasing the material modification. The lower degradation as a function of the ion bombardment has been also explained in the literature by the formation of a denser and oxidized surface: this densification induced by the ion bombardment is supposed to limit the diffusion of oxidizing species deep into the material.^{9,24} Indeed, in our experimental conditions, XRR analyses performed in Sec. III B 3 have also shown a denser film surface after RIE plasma treatments. However, the thickness of this layer is around ten times more important than the ion penetration depth, showing that the hypothesis presented in the above papers is not suitable in our case.

Furthermore, complementary ellipsometry measurements performed *in situ* and *ex situ* (after air exposure) on the hp-SiOCH after RIE-O₂ plasma, underline an increase in the refractive index of the film, assigned to a change in the film properties (see Fig. 9). This is related to the moisture absorption in the film after air exposure. This complementary study shows (i) that the film densification does not prevent species diffusion and (ii) that water uptake mechanisms proposed by Chang *et al.* in Eqs. (1) and (2) are enhanced not only by the ash process but also by the air exposure. Thus, contrary to the literature, our experiments show that the denser layer generated by the O₂ ash plasma does not prevent water molecule diffusion into the material. In summary, the ion bombardment does not play a significant role in the material degradation and cannot prevent the material modification in our experimental conditions.

2. Impact of the oxygen reactive species concentration on the film modification

In this section, the concentration of reactive species is increased by varying the source power from 200 to 800 W. The impact of these plasma conditions is investigated on raised coupons. Under these conditions, the floating samples are exposed to the oxygen flux of the plasma, while the im-

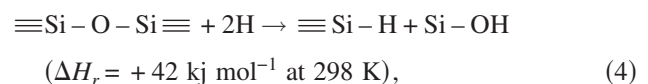
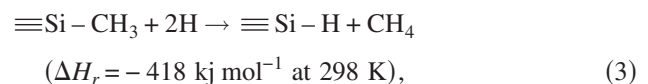
port of the ion energy is strongly minimized since the sample is floating. In these plasma conditions, the hp-SiOCH film consumptions are estimated at 16 and 3 nm when using 800 and 200 W, respectively. After exposure to oxidizing plasmas (200 and 800 W), FTIR spectra show in Fig. 8 that the broad adsorption band between 3000 and 3700 cm⁻¹ is unchanged, whatever the plasma power is. An important shift of the SiOSi peak to higher wave numbers (+20 cm⁻¹) is observed at 800 W source, which is related to a decrease of 73% in SiCH₃/SiOSi peak intensity area. When the plasma source power is decreased down to 200 W, the SiOSi shift is only +8 cm⁻¹, corresponding to a 33% methyl group consumption.

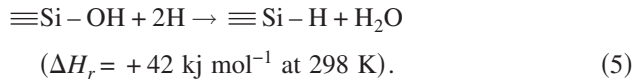
Based on the previous results presented in Sec. III B 3, we can consider that the film is modified deeper (related to the loss of methyl group) under plasma conditions performed at a higher plasma power (800 W) since the remaining hp-SiOCH film thickness is almost the same in both cases. Figure 8 also shows an increase in the SiOSi absorption band intensity when the plasma source power increases from 200 to 800 W. This behavior is in good agreement with the mechanism proposed by Chang *et al.* to explain the film modification [Eqs. (1) and (2)].²⁰ At 800 W, more oxygen radicals can react with the methyl groups present in the hp-SiOCH leading to a conversion of SiCH₃ into SiOH [Eq. (1)]. The formation of more SiOH groups leads to the formation of more SiOSi vibration modes [Eq. (2)]. Following this equation, H₂O formation is also expected. These results clearly show that the hp-SiOCH modified depth is strongly dependent on the concentration of oxygen reactive species in the plasma.

In this section, we have investigated the mechanisms of material modification with an O₂ plasma exposure. Oxygen radicals react with Si-CH₃ bonds and form CO₂, H₂O, and Si-OH bonds. Two silanol groups can cross-link together to give Si-O-Si structure with the simultaneous formation of water. These reactions are drastically depending on the oxygen species concentration in the plasma, while the ion bombardment energy does not play a significant role in the experimental conditions described in these studies.

B. H₂ plasma

The effect of hydrogen plasma on dense and porous dielectric film modifications has also been widely studied in the literature.^{8,21,25-27} The atomic hydrogen in the plasma can break bonds in the SiOCH matrix leading to the formation of more polar Si-H and Si-OH bonds, as listed in the potential following reactions:



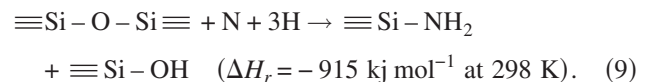
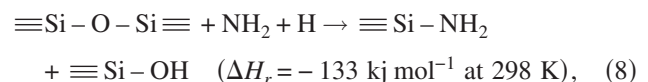
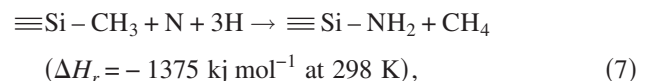
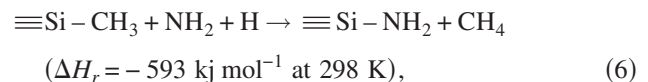


These reactions involve the formation of H_2O and CH_4 volatile by-products. Hydrogen species can react with $\text{Si}-\text{O}-\text{Si}$ and $\text{Si}-\text{CH}_3$ to form SiH_x and $\text{Si}-\text{OH}$ terminating bonds which can lead to a structural change of the SiOCH matrix. The enthalpy of reaction (3) is much lower than those of reactions (4) and (5), indicating that H atoms break more easily $\text{Si}-\text{CH}_3$ bonds than $\text{Si}-\text{O}$ bonds to preferentially form $\text{Si}-\text{H}$ bonds. In the literature, some studies have reported that the H_2 plasma treatment does not induce a film modification,^{3,4} while others have indicated that the film is damaged after H_2 plasma exposure.^{21,25,26,28} All these studies point out that the film modification is temperature dependent and is also correlated to the density of the H reactive species concentration in the plasma.²¹ The film damage is minimized by increasing the substrate temperature,^{25,26} while the damage is amplified with the reactive species concentration. Worsley *et al.* suggest that, at elevated temperatures, the concentration of H species chemisorbed at the surface decreases due a lower sticking coefficient and that the material modification is strongly dependent on the porosity rate and the interconnectivity of the pores.²¹ As for Lazzeri *et al.*,²⁸ the chemical damage introduced by H_2 -based discharges depends strongly on the formulation of the organosilicate material. The substrate temperature is also seen to affect the influx of plasma species (extent of material modifications). In our study, FTIR analyses (not shown) reveal no structural change (no bulk methyl group consumption and moisture uptake and no apparition of $\text{Si}-\text{H}$ bonds) and no increase of the dielectric constant after exposure to DS-H_2 plasma for both materials (lp- and hp- SiOCH materials). The only noticeable impact of the H_2 plasma is a slight carbon consumption detected at the lp- and hp- SiOCH surfaces by XPS (see Table III). The high substrate temperature at which the experiments are performed (270°C) can explain why the H_2 plasma does not induce any noticeable material modification even for the hp- SiOCH material. These results indicate that a H_2 downstream plasma treatment performed at a high substrate temperature may lead to optimal conditions to strip the photoresist and minimize the film degradation. Another study²⁹ has reported a strong bias dependence of the material modification in a H_2 plasma. Our experiments performed in downstream plasmas without ion bombardment and inducing no material modifications are in good agreement with this study.

It has to be noticed that after DS-O_2 plasma exposure, the hp- SiOCH is fully carbon depleted, as shown by FTIR [see Fig. 3(b)]. Based on the chemical reactions between H or O and hp- SiOCH , oxygen is more efficient to remove carbon species than hydrogen since the thermodynamic driving force for O induced modification of hp- SiOCH is more than twice as great as that for H atoms.^{21,29} This important difference in reactivity is well correlated with the difference in film modification observed between both chemistries (O_2 and H_2), although the thermodynamics does not dictate the kinet-

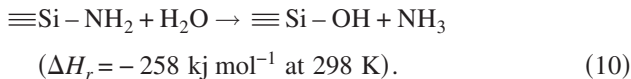
ics, and other parameters such as the density of reactive species present in the plasma must be considered.²¹

When He and Ar gases are added to H_2 , we have shown that the lp- and hp- SiOCH are hardly altered since no structural modifications are observed. Since Ar and He gas additions both contribute to improve the resist removing efficiency without degrading the low- k material, these gas mixtures (H_2/Ar and H_2/He) are promising ash chemistries. This result is in good agreement with the observations of Louveau *et al.*³ performed on patterned wafers since no difference in terms of film modification has been detected between H_2 and H_2/He ash plasmas. When N_2 is added to the DS-H_2 chemistry, only the surface is carbon depleted in the lp- SiOCH film, whereas a partial carbon depletion ($\sim 20\%$ with respect to the pristine film) is observed in the bulk of the hp- SiOCH with a significant moisture uptake. This result indicates that (i) the film modification depends on the porosity of the material and that (ii) N_xH_y , H, and N reactive radicals formed in such a gas mixture react with the SiOCH matrix leading to the modification observed. What is the impact of a pure DS-N_2 plasma on the SiOCH matrix? After exposure to DS-N_2 plasma, both lp- and hp- SiOCH are hardly altered since the film degradation only occurs at the film surface (see Table III). FTIR analyses (not shown) reveal no significant carbon depletion and moisture uptake. This shows that atomic nitrogen does not significantly react with the SiOCH matrix in such downstream plasma conditions. This result is in good agreement with Xu *et al.*, who have shown a very slight material modification using an inductive N_2 plasma. Based on these results, we can propose the possible reactions in a $\text{DS-N}_2/\text{H}_2$ plasma to explain the carbon depletion and silanol groups formation observed in the hp- SiOCH ,



These reactions involve the formation of volatile by-products such as CH_4 . Hydrogen species can react with $\text{Si}-\text{O}-\text{Si}$ and $\text{Si}-\text{CH}_3$ to form $\text{Si}-\text{NH}_2$ and $\text{Si}-\text{OH}$ terminating bonds which can lead to a structure change of the SiOCH matrix as observed for the hp- SiOCH . The enthalpy of reactions are much higher for reaction (6) than for reaction (8) and also for reaction (7) than for reaction (9), indicating that N and H atoms break $\text{Si}-\text{CH}_3$ bonds more easily than $\text{Si}-\text{O}$ bonds to preferentially form $\text{Si}-\text{NH}_2$ bonds. The enthalpy of reaction is also much lower than that without nitrogen, explaining the higher material modification in $\text{DS-N}_2/\text{H}_2$ plasmas than in

DS-H₂ plasmas. It has to be noticed that NH_x bonds are not evidenced on FTIR spectra, since their vibration energy is around 3335 cm⁻¹,³⁰ and then included into the moisture uptake broad absorption band. OSi-N are also not detected by FTIR, since their energy is between 874 and 1042 cm⁻¹,³⁰ and then masked by the Si-OH and SiOSi peaks. Nevertheless, the low amount of nitrogen observed by XPS indicates that few Si-NH₂ bonds are present on the top surface after plasma and air exposures. The non detection of NH_x bonds can be attributed by the reaction of water molecule with Si-NH₂ bonds when the wafer is exposed to the atmosphere,



Exposure of modified material to the atmosphere can then amplify the formation of silanol groups and decreases the amount of nitrogen into the modified top surface.

In the RIE mode using NH₃, no deep structural modification is evidenced for the lp-SiOCH material, whereas a partial carbon depletion and moisture uptake are observed for the hp-SiOCH material, showing again that the film modification depends on the porosity of the film. The material modification is similar to a DS-N₂/H₂ plasma in terms of carbon depletion, water uptake, and thickness of the damaged layer (~60 nm). In addition, *in situ* (not presented here) and *ex situ* XPS analyses after NH₃-RIE plasma treatment show that the nitrogen content on the top surface is strongly reduced after air exposure. It confirms reaction (10). This may indicate that the mechanisms leading to the material modification are probably the same for NH₃ as those presented for DS-N₂/H₂ plasma, although DS or RIE mode cannot be directly compared since the plasma characteristics are different.

C. Origin of the *k*-value degradation

After RIE-NH₃, RIE-O₂, and DS-N₂/H₂ plasma treatments, we have shown that the *k* value of the hp-SiOCH film increases from 2.2 up to 2.5, 2.8, and 3.2, respectively. At the same time, the different characterizations have revealed that our material is composed of a modified upper layer on top of a hardly modified material (with only a slight moisture uptake). The modified layer made of SiO_xN_yH_z after RIE-NH₃ and DS-N₂/H₂ or SiO_xH_y after RIE-O₂ RIE plasma is denser than the pristine material, carbon depleted, hydrophilic, and with a structural modification of the SiOSi structure. It is well-known that the dielectric constant increases with density, and that SiO_xN_yH_z or SiO_xH_y have a higher dielectric constant than a hp-SiOCH. We can, therefore, assume that the dielectric constant increase is mainly due to the upper layer. The contribution of the underneath material which exhibits characteristics close to the pristine material with a small amount of water uptake can be considered as negligible.

We can then assimilate the material after ashing as the addition of two dielectric materials associated in series. The capacitance of ash material by surface unit is then given by

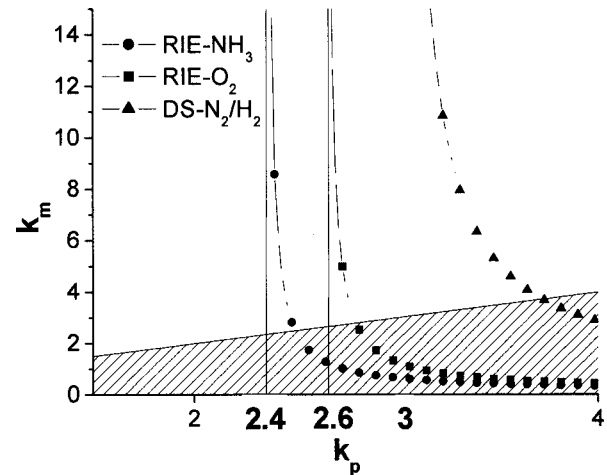


FIG. 10. Evolution of the dielectric constant from the modified material (k_m) vs dielectric constant of the unmodified material (k_p) for different plasma conditions.

$$C_{\text{eff}} = \frac{k_{\text{eff}}}{t} \varepsilon_0 = \left(\frac{t_m}{k_m} + \frac{t_p}{k_p} \right)^{-1} \varepsilon_0,$$

where k_{eff} is the effective *k* value, *t* the thickness of our layer, ε_0 the dielectric constant of the vacuum, t_m and k_m the thickness and dielectric constant of the modified material, and t_p and k_p those of the unmodified remaining material. In this equation, the only unknown variable is k_m , and we can then estimate it by

$$k_m = \frac{t_m}{t/k_{\text{eff}} - t_p/k_p}.$$

Using our data, the calculated dielectric constant is negative for RIE-NH₃, RIE-O₂, and DS-N₂/H₂, which is impossible. This indicates that our model is false. Therefore, the underneath layer which was supposed to have no impact on the *k* increase may have a higher dielectric constant than that of the pristine material. Figure 10 represents k_m vs k_p for the three different plasma treatments. The first bisecting is also represented in this figure in order to separate values where k_p is higher than k_m . We can see that the lowest possible values for k_p are 2.4, 2.6, and 3 for RIE-NH₃, RIE-O₂, and DS-N₂/H₂, respectively, showing that the ash plasma induces an increase of the underneath material *k* value which can be attributed to the moisture uptake. In previous studies, we have already shown that the moisture uptake has a huge impact on the increase of the dielectric constant.³¹ This moisture uptake can explain the increase of the *k* value of our material. Following the literature,³² one can estimate the amount of moisture uptake by decomposing the broad absorption peak between 2900 and 3800 cm⁻¹ into three peaks. The two lowest energy bands at 3300 and 3500 cm⁻¹ correspond directly to moisture uptake. The third one at 3650 cm⁻¹ is attributed to isolated silanols and then is not correlated with moisture uptake. The deconvolution has been performed using ORIGIN™ nonlinear curve fitting procedure. We have reported in Fig. 11 the evolution of the *k* value, the carbon depletion, and the moisture uptake on hp-SiOCH af-

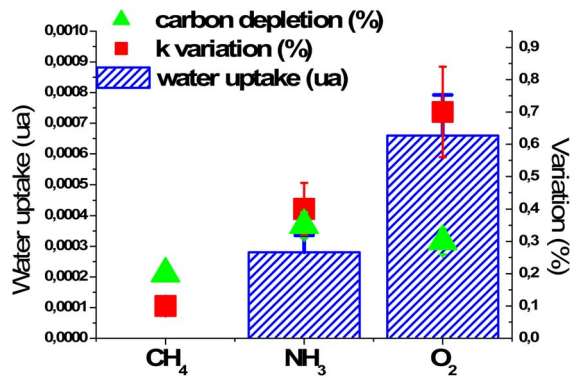


FIG. 11. Impact of the carbon depletion and moisture uptake on k -value variation as a function of ash plasma.

ter RIE-NH₃, RIE-O₂, and DS-N₂/H₂ plasmas. Previous published experimental data³¹ showing the impact of a CH₄-based ash chemistry on the hp-SiOCH film modification performed in a decoupled plasma source (DPS+) from Applied Materials (generating high density plasmas) have also been plotted. In this paper, we have shown that despite a 20% loss of the methyl groups, the k value is slightly impacted (+10%). This behavior is attributed and correlated with the absence of moisture absorption in the remaining porous material. Figure 11 figures out that the increase in k value is mainly related to moisture uptake rather than carbon depletion, whatever the plasma treatments are. After DS-N₂/H₂ ash plasma exposure, Fig. 11 shows higher moisture uptake and carbon depletion than in RIE chemistries. Both carbon consumption and moisture uptake lead to a strong increase in k value (+50%). After RIE ash chemistries (NH₃ and O₂), the carbon depletion is identical for both chemistries, while a higher water uptake is detected after O₂ plasma exposure compared to NH₃ chemistry. In this case, a higher k value is detected for the O₂ RIE plasma. This result is in good agreement with our previous study and highlights that the raise of the k value is mainly correlated with the amount of moisture uptake and less correlated with the carbon depletion.

V. CONCLUSION

The impact of reducing and oxidizing ash plasmas on porous SiOCH with varied porosities (8% and 45%) has been investigated on blanket wafers in RIE and DS modes. Opposite to the lp-SiOCH (8% porosity), where the film modification is limited at the surface, hp-SiOCH (45% porosity) is partially altered after exposure to DS-H₂/N₂ and both RIE chemistries (O₂ and NH₃) and even fully modified after oxidizing DS plasma exposure. No noticeable degradation is detected with nitrogen-free reducing DS chemistries (H₂/Ar and H₂/He). The porosity amplifies the sensitivity of the material to plasma treatments. FTIR analyses show higher carbon depletion and moisture uptake in the remaining hp-SiOCH film than in the lp-SiOCH, induced by the reactive species diffusion through the pores during the plasma exposure. In the case of oxidizing chemistry, oxygen reactive spe-

cies can deeply diffuse into the film and react with Si-CH₃ bonds to form CO₂, H₂O, and Si-OH bonds. These reactions are drastically depending on the oxygen species concentration in the plasma, while the ion bombardment does not play a significant role in our experimental conditions. In the case of a reducing chemistry, the atomic hydrogen in the plasma reacts with Si-O-Si and Si-CH₃ to form SiH_x and SiOH terminating bonds. Contrary to oxygen-based DS chemistries, the carbon depletion only occurs at the film surface with hydrogen chemistry, revealing an important difference in reactivity between both chemistries. Ar or He addition in hydrogen chemistry only contributes to increase the resist removal rate, while N₂ addition leads to the formation of Si-NH₂ and SiOH bonds which favors the water uptake after air exposure. Similar mechanisms leading to the material modification in terms of carbon depletion and water uptake can be depicted to the RIE-NH₃ chemistry.

These different reactions lead to the formation of a 40–60 nm modified layer composed of SiO_xN_yH_z after RIE-NH₃ and DS-N₂/H₂ or SiO_xH_y after RIE-O₂ plasmas which is denser, carbon depleted, hydrophilic, and with a structural modification. In our experimental conditions, the film densification does not prevent the water molecule diffusion and adsorption into the material. We have shown that the moisture uptake is the main factor responsible for an increase of the hp-SiOCH k value rather than the carbon depletion. These results underline that ashing chemistries have to preserve the hydrophobic nature of the low- k material to prevent k increase even with a strong carbon depletion.

¹International Technology Roadmap for Semiconductors, 2006 (<http://www.itrs.net/Links/2006Update/2006UpdateFinal.htm>).

²D. Shamiyan, M. R. Baklanov, S. Vanhaelemeersch, and K. Maex, *J. Vac. Sci. Technol. B* **20**, 1923 (2002).

³O. Louveau, C. Bourlot, A. Marfoure, I. Kalinovski, J. Su, G. H. Hills, and D. Louis, *Microelectron. Eng.* **73**, 351 (2004).

⁴A. Matsushita *et al.*, IITC Proceedings, 2003 (unpublished), p. 147.

⁵T. Mourier *et al.*, IITC Proceedings, 2003 (unpublished), p. 245.

⁶E. Ryan *et al.*, *Mater. Res. Soc. Symp. Proc.* **766** (2003).

⁷G. Beyer, A. Satta, J. Schumacher, K. Maex, W. Besling, O. Kipela, H. Sprey, and G. Tempel, *Microelectron. Eng.* **64**, 233 (2002).

⁸K. Yonekura, S. Sakamori, K. Goto, M. Matsuura, N. Fujiwara, and M. Yoneda, *J. Vac. Sci. Technol. B* **22**, 548 (2004).

⁹S. W. Hwang, G. R. Lee, J. H. Min, and S. Heup Moon, *Surf. Coat. Technol.* **174**, 835 (2003).

¹⁰L. G. Gosset *et al.*, Proceedings of the Advanced Metallization Conference, 2005 (AMC 2005) (unpublished), pp. 587–593.

¹¹F. Iacopi *et al.*, *J. Appl. Phys.* **99**, 053511 (2006).

¹²N. Posseme, T. Chevolleau, O. Joubert, L. Vallier, and P. Mangiagalli, *J. Vac. Sci. Technol. B* **21**, 2432 (2003).

¹³N. Posseme, T. Chevolleau, O. Joubert, L. Vallier, and N. Rochat, *J. Vac. Sci. Technol. B* **22**, 2772 (2004).

¹⁴C. Wyon, J. P. Gonchond, D. Delille, A. Michallet, J. C. Royer, L. Kwakman, and S. Marthon, *Appl. Surf. Sci.* **253**, 21 (2006).

¹⁵D. Rebiscoul, A. Van der Lee, P. Frugier, A. Ayrat, and S. Gin, *J. Non-Cryst. Solids* **325**, 113 (2003).

¹⁶J. Y. Kim, M. S. Hwang, Y.-H. Kim, H. J. Kim, and Y. Lee, *J. Appl. Phys.* **90**, 2469 (2001).

¹⁷A. Grill and D. A. Neumayer, *J. Appl. Phys.* **94**, 6697 (2003).

¹⁸L. M. Han, J. Pan, S. Chen, N. Balasubramanian, J. Shi, L. S. Wong, and P. D. Foo, *J. Electrochem. Soc.* **148**, F148 (2001).

¹⁹J. A. Theil, D. V. Tsu, M. W. Watkins, S. S. Kim, and G. Lukovsky, *J. Vac. Sci. Technol. A* **8**, 1374 (1990).

- ²⁰T. C. Chang *et al.*, *J. Vac. Sci. Technol. B* **20**, 1561 (2002).
- ²¹M. A. Worsley, S. F. Bent, S. M. Gates, N. C. Fuller, W. Volksen, M. Steen, and T. Dalton, *J. Vac. Sci. Technol. B* **23**, 395 (2005).
- ²²O. Joubert, G. Cunge, B. Pelissier, L. Vallier, M. Kogelschatz, and E. Pargon, *J. Vac. Sci. Technol. A* **22**, 553 (2004).
- ²³T. Chevolleau, M. Darnon, T. David, N. Posseme, J. Torres, and O. Joubert, *J. Vac. Sci. Technol. B* **25**, 886 (2007).
- ²⁴E. Kondoh, T. Asano, A. Nakashima, and M. Komatu, *J. Vac. Sci. Technol. B* **18**, 1276 (2000).
- ²⁵A. Grill, V. Sternhagen, D. Neumayer, and V. Patel, *J. Appl. Phys.* **98**, 074502 (2005).
- ²⁶X. Hua *et al.*, *J. Vac. Sci. Technol. B* **24**, 1238 (2006).
- ²⁷A. Humbert, L. Mage, C. Goldberg, K. Junker, L. Proenca, and J. B. Lhuillier, *Microelectron. Eng.* **82**, 399 (2005).
- ²⁸P. Lazzeri, G. J. Stueber, G. S. Oehrlein, R. McGowan, E. Busch, S. Pederzoli, M. Bersani, and M. Anderle, *J. Vac. Sci. Technol. B* **24**, 2695 (2006).
- ²⁹S. Xu *et al.*, *J. Vac. Sci. Technol. B* **25**, 156 (2007).
- ³⁰J. Olivares-Roza, O. Sanchez, and J. M. Albella, *J. Vac. Sci. Technol. A* **16**, 2757 (1998).
- ³¹N. Posseme, T. David, T. Chevolleau, and O. Joubert, *Electrochem. Solid-State Lett.* **8**, G112 (2005).
- ³²A. Goulet, C. Vallée, A. Garnier, and G. Turban, *J. Vac. Sci. Technol. A* **18**, 2452 (2000).